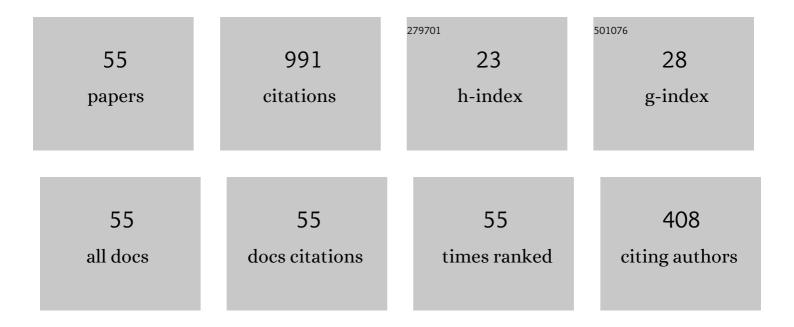
## **Oleg O Shichalin**

List of Publications by Year in descending order

Source: https://exaly.com/author-pdf/3564542/publications.pdf

Version: 2024-02-01



#	Article	IF	CITATIONS
1	Synthesis of amorphous KAlSi3O8 for cesium radionuclide immobilization into solid matrices using spark plasma sintering technique. Ceramics International, 2022, 48, 3808-3817.	2.3	33
2	Comparative study of WC-based hard alloys fabrication via spark plasma sintering using Co, Fe, Ni, Cr, and Ti binders. International Journal of Refractory Metals and Hard Materials, 2022, 102, 105725.	1.7	25
3	Fast (Ce,Gd) <sub>3</sub> Ga <sub>2</sub> Al <sub>3</sub> O <sub>12</sub> Scintillators Grown by the Optical Floating Zone Method. Crystal Growth and Design, 2022, 22, 180-190.	1.4	11
4	Rabbit's cranial defect regeneration using a fine-grained ZrO2- (15Âwt%)HAp ceramic implant fabricated by SPS-RS technique. Ceramics International, 2022, 48, 13817-13825.	2.3	1
5	Hydrothermal synthesis and spark plasma sintering of NaY zeolite as solid-state matrices for cesium-137 immobilization. Journal of the European Ceramic Society, 2022, 42, 3004-3014.	2.8	39

6 Wide Concentration Range of Tb3+ Doping Influence on Scintillation Properties of (Ce, Tb,) Tj ETQq0 0 0 rgBT /Overlock 10 Tf 50 542 To

7	Reaction synthesis of SrTiO3 mineral-like ceramics for strontium-90 immobilization via additional in-situ synchrotron studies. Ceramics International, 2022, 48, 19597-19605.	2.3	14
8	A novel approach for rice straw agricultural waste utilization: Synthesis of solid aluminosilicate matrices for cesium immobilization. Nuclear Engineering and Technology, 2022, 54, 3250-3259.	1.1	24
9	Hydrothermal synthesis, structure and sorption performance to cesium and strontium ions of nanostructured magnetic zeolite composites. Nuclear Engineering and Technology, 2022, 54, 1991-2003.	1.1	23
10	Synthesis and spark plasma sintering of solid-state matrices based on calcium silicate for 60Co immobilization. Journal of Alloys and Compounds, 2022, 912, 165233.	2.8	9
11	Synthesis of Ti-Cu Multiphase Alloy by Spark Plasma Sintering: Mechanical and Corrosion Properties. Metals, 2022, 12, 1089.	1.0	8
12	Ce3+ doped Lu3Al5O12 ceramics prepared by spark plasma sintering technology using micrometre powders: Microstructure, luminescence, and scintillation properties. Journal of the European Ceramic Society, 2022, 42, 6663-6670.	2.8	10
13	UO2-Eu2O3 compound fuel fabrication via spark plasma sintering. Journal of Alloys and Compounds, 2021, 854, 155904.	2.8	6
14	A novel IR-transparent Ho3+:Y2O3–MgO nanocomposite ceramics for potential laser applications. Ceramics International, 2021, 47, 1399-1406.	2.3	6
15	WC-5TiC-10Co hard metal alloy fabrication via mechanochemical and SPS techniques. International Journal of Refractory Metals and Hard Materials, 2021, 94, 105385.	1.7	31
16	Influence of sintering parameters on transparency of reactive SPSed Nd3+:YAG ceramics. Optical Materials, 2021, 112, 110760.	1.7	12
17	Al2O3–Ce:YAG and Al2O3–Ce:(Y,Gd)AG composite ceramics for high brightness lighting: Effect of microstructure. Materials Characterization, 2021, 172, 110883.	1.9	27
18	SrAl2Si2O8 ceramic matrices for 90Sr immobilization obtained via spark plasma sintering-reactive synthesis. Nuclear Engineering and Technology, 2021, 53, 2289-2294.	1.1	29

OLEG O SHICHALIN

#	Article	IF	CITATIONS
19	Synthetic nanostructured wollastonite: Composition, structure and "in vitro―biocompatibility investigation. Ceramics International, 2021, 47, 22487-22496.	2.3	9
20	Reactive SPS of Nd :YAG transparent ceramics with LiF sintering additive. Optical Materials, 2021, 119, 111389.	1.7	4
21	UO2–Y2O3 ceramic nuclear fuel: SPS fabrication, physico-chemical investigation and neutron absorption evaluation. Journal of Alloys and Compounds, 2021, 877, 160266.	2.8	3
22	Al2O3–Ce:YAG composite ceramics for high brightness lighting: Cerium doping effect. Journal of Alloys and Compounds, 2021, 887, 161486.	2.8	8
23	SPS hard metal alloy WC-8Ni-8Fe fabrication based on mechanochemical synthetic tungsten carbide powder. Journal of Alloys and Compounds, 2020, 816, 152547.	2.8	25
24	Influence of sintering temperature on structural and optical properties of Y2O3–MgO composite SPS ceramics. Ceramics International, 2020, 46, 6537-6543.	2.3	33
25	Morphological Characteristics of the Osteoplastic Potential of Synthetic CaSiO3/HAp Powder Biocomposite. Journal of Functional Biomaterials, 2020, 11, 68.	1.8	6
26	Phase Formation and Densification Peculiarities of Hf–C–N Solid Solution Ceramics during Reactive Spark Plasma Sintering. Advanced Engineering Materials, 2020, 22, 2000482.	1.6	13
27	Spark plasma sintering-reactive synthesis of SrWO4 ceramic matrices for 90Sr immobilization. Vacuum, 2020, 180, 109628.	1.6	24
28	Synthesis and Spark Plasma Sintering of Microcrystalline Thorium Dioxide for Nuclear Fuel Products. Russian Journal of Inorganic Chemistry, 2020, 65, 1245-1252.	0.3	3
29	CaSiO3-HAp Structural Bioceramic by Sol-Gel and SPS-RS Techniques: Bacteria Test Assessment. Journal of Functional Biomaterials, 2020, 11, 41.	1.8	7
30	Spark plasma sintering of UO2 fuel composite with Gd2O3 integral fuel burnable absorber. Nuclear Engineering and Technology, 2020, 52, 1756-1763.	1.1	9
31	Sol-gel (template) synthesis of osteoplastic CaSiO3/HAp powder biocomposite: "In vitro―and "in vivo― biocompatibility assessment. Powder Technology, 2020, 367, 762-773.	2.1	25
32	Synthesis of Hf-C-N ceramics by spark plasma sintering. EPJ Web of Conferences, 2019, 196, 00012.	0.1	2
33	Synthesis of BaCe0.9xZrxY0.1O3 nanopowders and the study of proton conductors fabricated on their basis by low-temperature spark plasma sintering. International Journal of Hydrogen Energy, 2019, 44, 20345-20354.	3.8	37
34	Sol-gel synthesis of SiC@Y3Al5O12 composite nanopowder and preparation of porous SiC-ceramics derived from it. Materials Chemistry and Physics, 2019, 235, 121734.	2.0	12
35	ZrO2-phosphates porous ceramic obtained via SPS-RS "in situ―technique: Bacteria test assessment. Ceramics International, 2019, 45, 13838-13846.	2.3	12
36	SPS technique for ionizing radiation source fabrication based on dense cesium-containing core. Journal of Hazardous Materials, 2019, 369, 25-30.	6.5	34

OLEG O SHICHALIN

#	Article	IF	CITATIONS
37	Influence of vacuum heating on magnetic characteristics of α-Fe2O3 ceramics obtained via spark plasma sintering. , 2019, , .		0
38	Spark Plasma Sintering of Special-Purpose Functional Ceramics Based on UO2, ZrO2, Fe3O4/α-Fe2O3. Glass Physics and Chemistry, 2018, 44, 632-640.	0.2	27
39	Fabrication of highly-doped Nd3+:YAG transparent ceramics by reactive SPS. Ceramics International, 2018, 44, 23145-23149.	2.3	30
40	A complex approach to assessing porous structure of structured ceramics obtained by SPS technique. Materials Characterization, 2018, 145, 294-302.	1.9	42
41	Spark plasma sintering of nanopowders in the CeO2-Y2O3 system as a promising approach to the creation of nanocrystalline intermediate-temperature solid electrolytes. Ceramics International, 2018, 44, 19879-19884.	2.3	28
42	Synthesis of nanostructured iron oxides and new magnetic ceramics using sol-gel and SPS techniques. AIP Conference Proceedings, 2017, , .	0.3	5
43	Sol-gel and SPS combined synthesis of highly porous wollastonite ceramic materials with immobilized Au-NPs. Ceramics International, 2017, 43, 8509-8516.	2.3	27
44	Preparation of porous SiC-ceramics by sol–gel and spark plasma sintering. Journal of Sol-Gel Science and Technology, 2017, 82, 748-759.	1.1	29
45	Spark Plasma Sintering as a high-tech approach in a new generation of synthesis of nanostructured functional ceramics. Nanotechnologies in Russia, 2017, 12, 49-61.	0.7	30
46	Behavior of HfB2-SiC (10, 15, and 20 vol %) ceramic materials in high-enthalpy air flows. Russian Journal of Inorganic Chemistry, 2016, 61, 1203-1218.	0.3	29
47	Wollastonite ceramics with bimodal porous structures prepared by sol–gel and SPS techniques. RSC Advances, 2016, 6, 34066-34073.	1.7	15
48	Behavior of a sample of the ceramic material HfB2–SiC (45 vol %) in the flow of dissociated air and the analysis of the emission spectrum of the boundary layer above its surface. Russian Journal of Inorganic Chemistry, 2015, 60, 1360-1373.	0.3	32
49	Application of carbonaceous template for porous structure control of ceramic composites based on synthetic wollastonite obtained via Spark Plasma Sintering. Ceramics International, 2015, 41, 1171-1176.	2.3	27
50	HfB2-SiC (10–20 vol %) ceramic materials: Manufacture and behavior under long-term exposure to dissociated air streams. Russian Journal of Inorganic Chemistry, 2014, 59, 1361-1382.	0.3	29
51	HfB2-SiC (45 vol %) ceramic material: Manufacture and behavior under long-term exposure to dissociated air jet flow. Russian Journal of Inorganic Chemistry, 2014, 59, 1298-1311.	0.3	29
52	Production of ultrahigh temperature composite materials HfB2-SiC and the study of their behavior under the action of a dissociated air flow. Russian Journal of Inorganic Chemistry, 2013, 58, 1269-1276.	0.3	30
53	Synthesis of Ceramic and Glass Ceramic Matrices with Immobilized Cesium Radionuclides for Active Zones of Ionizing Radiation Sources. Materials Science Forum, 0, 945, 827-832.	0.3	1
54	Stable growth of (Ce,Cd)3Ga2Al3O12 crystal scintillators by the traveling solvent floating zone method. CrystEngComm, 0, , .	1.3	1

#	Article	IF	CITATIONS
55	Adsorption of Co(II) ions using Zr-Ca-Mg and Ti-Ca-Mg phosphates: adsorption modeling and mechanistic aspects. Environmental Science and Pollution Research, O, , .	2.7	3